

# Photoelectron Spectroscopic Analysis of Through-Bond Interaction via Cyclobutane Relay Orbitals. Evidence for Strong Relay Conjugation in Tricyclo[5.5.0.0<sup>2,8</sup>]dodecatetraene

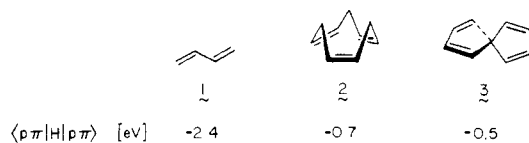
Rolf Gleiter,\*<sup>1a</sup> Azumao Toyota,<sup>1a</sup> Peter Bischof,<sup>1a</sup> Gerhard Krennrich,<sup>1a</sup> Jürgen Dressel,<sup>1b,2</sup> Paul D. Pansegrau,<sup>1b</sup> and Leo A. Paquette\*<sup>1b</sup>

Contribution from the Institut für Organische Chemie der Universität Heidelberg, D-6900 Heidelberg, West Germany, and Evans Chemical Laboratories, The Ohio State University, Columbus, Ohio 43210. Received December 3, 1987

**Abstract:** In a first series of experiments, the He ( $I_{\alpha}$ ) photoelectron (PE) spectra of tricyclo[5.5.0.0<sup>2,8</sup>]dodecatetraene (**4**), tricyclo[5.5.0.0<sup>2,8</sup>]dodeca-3,5-diene (**5**), and tricyclo[5.5.0.0<sup>2,8</sup>]dodecane (**6**) were recorded. The assignments to their first PE bands are based on correlation and molecular orbital (MO) calculations. For **4**, the sequence of its highest occupied MO's is  $11_1(\pi)$ ,  $1a_2(\pi)$ , and  $7e(\pi)$ . The split between the first two bands amounts to 1.44 eV and is larger than that in spiro[4.4]nonatetraene. Quantitative analysis of the through-bond interaction between the four-membered relay and the peripheral  $\pi$  system points to the existence of a strong interaction between  $b_1(\pi)$  and  $b_1(\sigma)$ . The observation that the split between the first two PE bands,  $\Delta I(1,2)$ , is nearly equal to the split of the first two bands in the electronic spectrum,  $\Delta E(1,2)$ , is explained in terms of analytical MO theory. A second group of experiments involved the PE spectra of tricyclo[5.3.0.0<sup>2,8</sup>]deca-3,5,9-triene (**13**), tricyclo[5.3.0.0<sup>2,8</sup>]deca-3,5-diene (**15**), and tricyclo[5.3.0.0<sup>2,8</sup>]dec-9-ene (**16**), as well as 9,10-dimethylenetricyclo[5.3.0.0<sup>2,8</sup>]deca-3,5-diene (**17**). Comparison of the PE spectra recorded for **13**, **15**, and **16** reveals the absence of interaction between the two olefinic fragments in **13**. Notable in the first bands of the PE spectra of **4** and **17** is a considerably smaller split between bands 1 and 2 in the case of **17** (1.10 eV) relative to **4** (1.44 eV). This phenomenon has been rationalized as due to the different connectivity between the central ring and the butadiene moieties. The electronic absorption spectrum of **17** has been investigated and interpreted by comparison with the results of CNDO/s-CI calculations.

A widely accepted procedure for acquiring a measure of electronic interactions within organic molecules and an approximation of their resulting impact on spectroscopic and chemical properties is based on the following scheme. A molecule containing two or more interacting moieties is split into model fragments, where the interacting systems are isolated from each other, and each is described in terms of "fragment molecular orbitals". Use of simple perturbational theory<sup>3</sup> then allows determination of appropriate interaction parameters, which in turn yield the best fit within the molecular orbital pattern of the molecule under study. Provided that Koopmans' theorem<sup>4</sup> holds, the reliability of the method can subsequently be checked by comparing the predictions with the results of photoelectron spectroscopy on a series of structurally related molecules. This procedure allows interpretation of a large amount of spectroscopic data starting from a reasonable number of model fragments and has further substantiated our understanding of electron molecular structure.

As an example, the procedure consistently yields a value for the interaction parameter  $\langle 2p\pi | H | 2p\pi \rangle$  of -2.4 eV for directly conjugated  $\pi$  bonds as in butadiene (**1**).<sup>5</sup> For the homoconjugation in *cis,cis,cis*-cyclononatriene (**2**), the interaction parameter amounts to -0.7 eV.<sup>6</sup> If the two  $\pi$  fragments are kept perpendicular by an  $sp^3$ -hybridized center as in spiro[4.4]nonatetraene (**3**), the interaction parameter is similar to that determined for



**2** (see below). This result is anticipated, since in  $\pi$  systems like **3** the overlap integral between two  $2p\pi$  AO's at positions 1, 4, 1', and 4' is close to that of **2**. The order of magnitude of  $\langle p | H | p \rangle$  listed for **2** and **3** has been confirmed for several homoconjugated and spiroconjugated systems by using PE spectroscopic analysis. On the basis of model calculations, it was previously postulated<sup>8</sup> that the interaction between two perpendicular  $\pi$  systems found in spiro compounds should be larger when their central carbon atom is replaced by a four-membered ring system as shown in Figure 1. This concept involves the replacement of the through-space interaction element in the spiro compound<sup>9</sup> by a through-bond interaction feature<sup>10</sup> in the resulting tricyclic system.

Proper comparison between the  $\pi$  orbitals of a spiro system such as **3** with those of four-membered ring Walsh orbitals<sup>11</sup> reveals a perfect matching (Figure 2). Calculations on several tricyclic model systems<sup>8</sup> predict a larger split between  $a_2$  and  $b_1$  than in the spiro system and a reversal of the sequence as shown in Figure 1. In line with these predictions are the results of experiments with electronic absorption and PE spectroscopy. Investigation of the electronic absorption spectrum of tricyclo[3.3.0.0<sup>2,6</sup>]octa-3,7-diene<sup>12</sup> and comparison of the electronic absorption spectra of 9,9'-spirobifluorene and tetrabenzotricyclo[5.5.0.0<sup>2,8</sup>]dodeca-3,5,9,11-tetraene<sup>13</sup> have given evidence for a large through-bond interaction between the two  $\pi$  moieties. When the PE spectra of tetravinylmethane and *trans,trans,trans*-1,2,3,4-tetravinylcyclobutane<sup>14</sup> are compared, a larger split between the  $b_1$  and  $a_2$

(7) Batich, C.; Heilbronner, E.; Rommel, E.; Semmelhack, M. F.; Foos, J. S. *J. Am. Chem. Soc.* **1974**, *96*, 7662.

(8) Bischof, P.; Gleiter, R.; Haider, R. *J. Am. Chem. Soc.* **1978**, *100*, 1036.

(9) Simmons, H. E.; Fukunaga, T. *J. Am. Chem. Soc.* **1967**, *89*, 5208. Hoffmann, R.; Imamura, A.; Zeiss, G. D. *Ibid.* **1967**, *89*, 5215. Dürr, H.; Gleiter, R. *Angew. Chem.* **1978**, *90*, 591; *Angew. Chem., Int. Ed. Engl.* **1978**, *17*, 559 and references therein.

(10) Hoffmann, R.; Imamura, A.; Hehre, W. J. *J. Am. Chem. Soc.* **1968**, *90*, 1499. Hoffmann, R. *Acc. Chem. Res.* **1981**, *4*, 1. Gleiter, R. *Angew. Chem.* **1974**, *86*, 770; *Angew. Chem., Int. Ed. Engl.* **1974**, *13*, 696. Padon-Row, M. N. *Acc. Chem. Res.* **1982**, *15*, 245 and references therein.

(11) Hoffmann, R.; Davidson, R. B. *J. Am. Chem. Soc.* **1971**, *93*, 5699. Salem, L.; Wright, J. S. *Ibid.* **1969**, *91*, 5947.

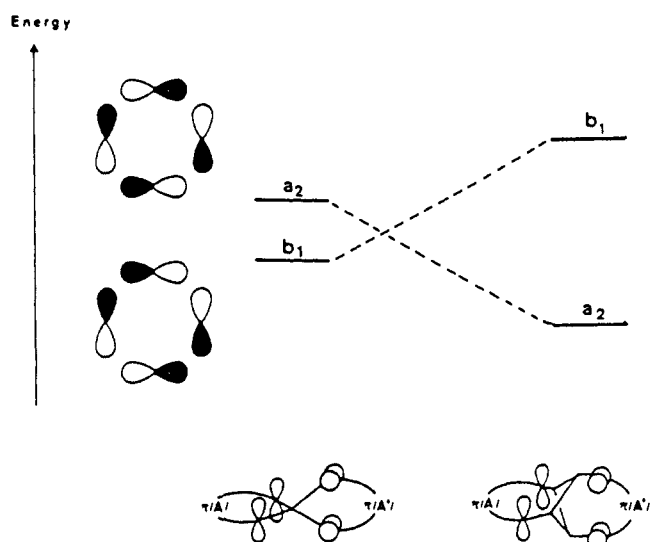
(12) Gleiter, R.; Kobayashi, T. *Helv. Chim. Acta* **1971**, *54*, 1081.

(13) Spanget-Larsen, J.; Gleiter, R.; Haider, R. *Helv. Chim. Acta* **1983**, *66*, 1441.

(1) (a) Universität Heidelberg. (b) The Ohio State University.  
 (2) Fulbright Scholar, 1982-1983; Evans Fellow, 1985-1986.  
 (3) (a) Heilbronner, E.; Bock, H. *Das HMO-Modell und seine Anwendung*; Verlag: Weinheim, 1970. (b) Dewar, M. J. S.; Dougherty, R. C. *The PMO Theory of Organic Chemistry*; Plenum: New York, 1975.  
 (4) Koopmans, T. *Physica (Utrecht)* **1934**, *1*, 104.  
 (5) Heilbronner, E.; Gleiter, R.; Hopf, H.; Hornung, V.; de Meijere, A. *Helv. Chim. Acta* **1971**, *54*, 783. Brogli, F.; Heilbronner, E. *Theor. Chim. Acta* **1972**, *26*, 289.  
 (6) Bischof, P.; Gleiter, R.; Heilbronner, E. *Helv. Chim. Acta* **1970**, *53*, 1425.

**Table I.** Comparison between the First Vertical Ionization Energies ( $I_{v,j}$ ) of 4–6 with Calculated Orbital Energies ( $\epsilon_j$ ) Based on FMO, MINDO/3, and ab Initio (STO-3G) Procedures<sup>a</sup>

compd	band	$I_{v,j}$	assignment	$-\epsilon_j$ (FMO)	$-\epsilon_j$ (MINDO/3)	$-\epsilon_j$ (STO-3G)
4	1	7.56	2b <sub>1</sub>	7.60	8.03	5.79
	2	9.00	1a <sub>2</sub>	8.50	9.13	7.21
	3	10.0	7e	10.03	9.77	9.40
	4	10.4				
	5	10.9	7a <sub>1</sub>		10.11	10.02
	6	11.1	6e	11.46	10.80	11.08
3	1	8.38	4a <sub>2</sub>	8.08	8.23	6.37
	2	10.2	8b <sub>1</sub>	9.90	9.58	9.40
	3	10.9	7b <sub>1</sub>	10.40	9.81	9.65
			13a <sub>1</sub>	10.40	9.88	10.36
6	1	9.6	7a <sub>1</sub>		10.07	9.41
	2	10.0	8e		9.75	9.43

<sup>a</sup> All values are in electronvolts.**Figure 1.** Orbital sequence for b<sub>1</sub> and a<sub>2</sub> in spiro compounds (left) and the corresponding tricyclic compounds (right).

	A <sub>1</sub>	A <sub>2</sub>	B <sub>1</sub>	B <sub>2</sub>	E

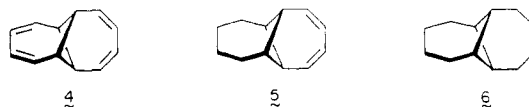
**Figure 2.** Comparison between the valence orbitals of a spiro system with the valence (Walsh) orbitals of cyclobutane.

band is clearly noted on the side of the cyclobutane derivatives. All of these investigations point up an excellent relay capacity for the four-membered ring system. An empirical treatment using a fragment molecular orbital approach yields a value of  $-1.9$  eV for the interaction parameter describing the interaction of a  $2p\pi$  AO of the vinyl group and a  $2p$  AO of the four-membered ring.<sup>14–17</sup> The recent synthesis of tricyclo[5.5.0.0<sup>2,8</sup>]dodecatetraene (**4**)<sup>18</sup> enables us to compare the electronic structure of **4** with that of

**Table II.** Comparison of the First Two PE Bands in **5** and **9–11**

compd	$I_{v,1}$	$I_{v,2}$	$I_{v,2} - I_{v,1}$
<b>5</b>	8.38	10.2	1.8
<b>9</b>	8.11	10.15	2.04
<b>10</b>	7.96	9.86	1.90
<b>11</b>	7.80	9.42	1.62

**3** and thus provides us with an ideal model to test theoretical predictions.



**PE Spectroscopic Investigation of 4–6.** The PE spectra of **4** and its more saturated congeners **5** and **6** are illustrated in Figure 3. The first ionization energies of all three compounds are listed in Table I. While several strongly overlapping bands starting around 9.6 eV are seen for **6**, one band at 8.4 and a shoulder at 10.3 eV appear in the spectrum of **5** followed by strongly overlapping bands near 11 eV. For **4**, two bands with a steep onset at 7.56 and 9.00 eV are encountered, well separated from a series of strongly overlapping bands at 10.0, 10.4, and 10.9 eV.

To interpret the PE spectra of **4–6**, the first PE bands are examined relative to those of related species. A simple fragment molecular orbital (FMO) model is then applied as mentioned in the introduction and, finally, the first ionization energies are compared with calculated orbital energies by using the MINDO/3 method<sup>19</sup> or a minimum basis (STO-3G) ab initio procedure.<sup>20</sup> The validity of Koopmans' theorem<sup>4</sup> is universally assumed for the compounds in question. The PE spectrum of **6**, when evaluated alongside those recorded for tricyclo[3.3.0.0]octane (**7**)<sup>16</sup> and tricyclo[5.3.0.0<sup>2,8</sup>]deca-3,5-diene (**8**)<sup>21</sup> suggests assignment of the first bands to ionization events from Walsh-type orbitals.<sup>11</sup> This conclusion is confirmed by results derived from those calculations listed in Table I.

Comparison of the PE data for **5** with those of bicyclo[4.1.1]octadiene (**9**),<sup>16</sup> tricyclo[5.3.0.0<sup>2,8</sup>]deca-3,5-diene (**10**),<sup>20</sup> and 1-methyltricyclo[5.5.0.0<sup>2,8</sup>]dodeca-3,5-diene (**11**)<sup>21</sup> (Table II) suggests that the first two bands of **5** be assigned to ionizations stemming from a<sub>2</sub>( $\pi$ ) and b<sub>1</sub>( $\pi$ ). In line with this assignment are results obtained using the FMO model (see below) and MO calculations (Table I). As concerns **4**, its bands 1–4 are logically assigned to ionization from  $\pi$  MO's. While the first two bands are split by 1.4 eV, bands 3 and 4 overlap strongly. The energy difference between the latter bands is ascribed to a Jahn–Teller split.

(14) Gleiter, R.; Haider, R.; Bischof, P.; Lindner, H. J. *Chem. Ber.* **1983**, *116*, 3736.(15) Bischof, P.; Gleiter, R.; de Meijere, A.; Meyer, L. U. *Helv. Chim. Acta* **1974**, *57*, 1519. Gleiter, R.; Bischof, P.; Gubernator, K.; Christl, M.; Schwager, L.; Vogel, P. *J. Org. Chem.* **1985**, *50*, 5064.(16) Bischof, P.; Gleiter, R.; Kukla, M. J.; Paquette, L. A. *J. Electron Spectrosc. Relat. Phenom.* **1974**, *4*, 177.(17) Gleiter, R.; Bischof, P.; Volz, W. E.; Paquette, L. A. *J. Am. Chem. Soc.* **1977**, *99*, 8.(18) (a) Paquette, L. A.; Dressel, J.; Chasey, K. L. *J. Am. Chem. Soc.* **1986**, *108*, 512. (b) Dressel, J.; Chasey, K. L.; Paquette, L. A. *J. Am. Chem. Soc.*, preceding paper in this issue.(19) Bingham, R. C.; Dewar, M. J. S.; Lo, D. H. *J. Am. Chem. Soc.* **1975**, *97*, 1285. The MINDO/3 UHF version written by P. Bischof (*J. Am. Chem. Soc.* **1976**, *98*, 6844) was utilized in this work.(20) Hehre, W. J.; Ditchfield, R.; Stewart, R. F.; Pople, J. A. *J. Chem. Phys.* **1970**, *52*, 2769.(21) Gleiter, R.; Sander, W.; Butler-Ransohof, I. *Helv. Chim. Acta* **1986**, *69*, 1872.

(22) Gleiter, R.; Butler-Ransohof, I., unpublished results.

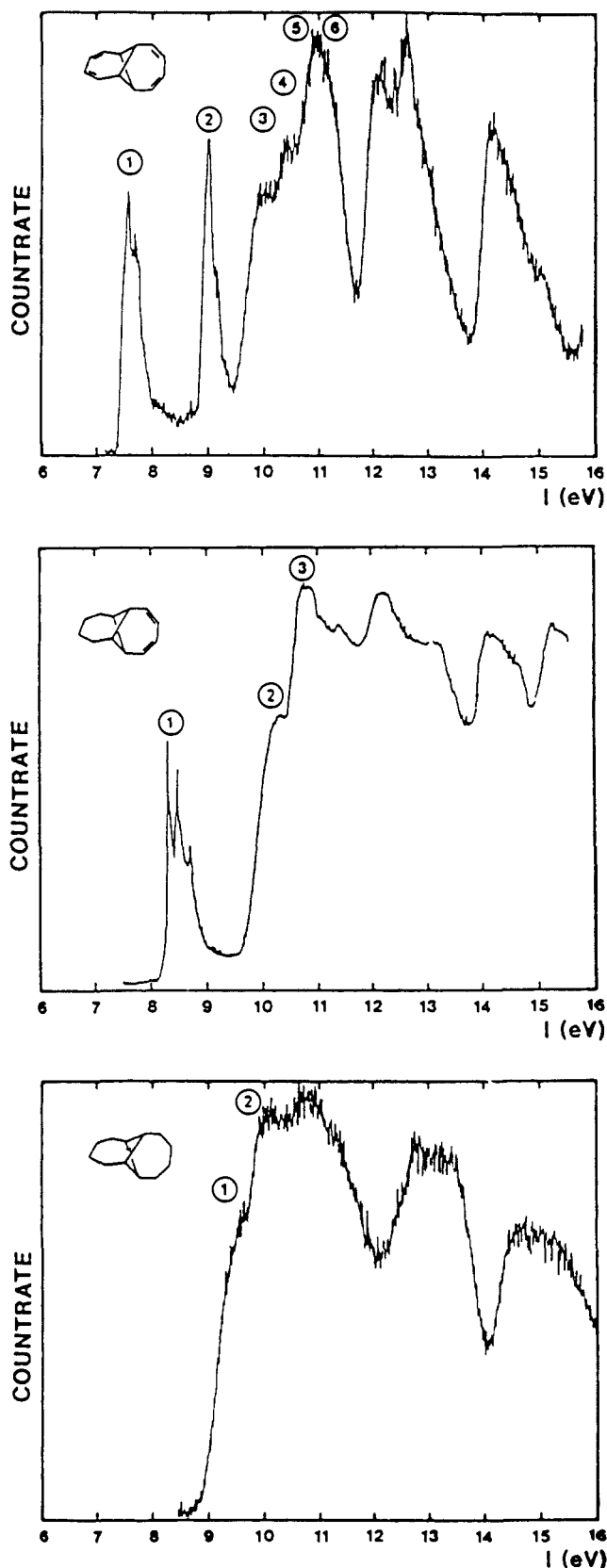


Figure 3. He ( $I_{\alpha}$ ) PE spectra of 4-6.

**Calculations for 4-6.** To enable proper assignment of the PE spectra of 4-6, we have carried out calculations of various types: an FMO model as described below, the MINDO/3 method,<sup>19</sup> and a minimum basis (STO-3G) ab initio procedure.<sup>20</sup> Since precise structural information for 4-6 is not available, these data were derived by minimization of each total energy with respect to all geometrical parameters by using the MINDO/3 method. Tetraene 4 has previously been analyzed in this fashion.<sup>8</sup> For the

symmetry	PCMO( $\pi$ )	CMO	PCMO( $\sigma$ )	$\langle \pi   F   \sigma \rangle$ (eV)
e				-0.60
b <sub>1</sub>				-2.35

Figure 4. Definition of the symmetry adapted precanonical  $\pi$  MO's (PCMO's) of the  $\pi$  fragments (second column from the left) and of the central ring unit (fourth column from left). The canonical MO's are shown in the third column and the matrix elements  $\langle \pi | F | \sigma \rangle$  between the PCMO's are given in the fifth column.

FMO approach to 4 ( $D_{2d}$ ), the following previously utilized<sup>15-17</sup> parameters were chosen:

$$\text{cyclobutane: } \epsilon(e) = -10.6 \text{ eV} \quad \epsilon(b_1) = -12.2 \text{ eV}$$

$$\text{butadiene: } \epsilon(b_1) = \epsilon(a_2) = -8.5 \text{ eV}$$

The interaction parameter assumed was  $\langle p\pi | H | p\sigma \rangle = -1.9 \text{ eV}$ . Importantly, the FMO model neglects any interaction between  $a_2(\pi)$  and  $a_2(\sigma^*)$ .

The outcome of these calculations is given in Table I. All methods agree to the extent that the same orbital sequence is predicted for the highest occupied MO's. The split of the first two peaks is found to be underestimated by the FMO and MINDO/3 procedures. The  $\pi$ - $\sigma$  interaction prevailing in 4 was analyzed by a method proposed by Heilbronner and Schmelzer<sup>23</sup> for the quantitative analysis of through-bond effects. In the first step, the occupied canonical MO's (CMO's) of the diagonal Fock matrix are transformed into a set of localized MO's (LMO's) by means of the Edmiston-Ruedenberg<sup>24</sup> procedure. In the non-diagonal Fock matrix of the LMO's, the off-diagonal element  $F_{\lambda,ij}$  provides a measure of the through-space interaction within the LMO's  $\lambda_i$  and  $\lambda_j$ . Diagonalization of selected substances defined by the  $\lambda_i$ 's leads to orbitals of canonical form, while taking into account certain through-space interactions. To determine the through-bond interaction quantitatively, a representation  $\Psi_i$  is needed of the one-particle space in which selected localized orbitals  $\lambda_i$  have nonvanishing interaction elements,  $F_{\Psi,ij}$ , to orbitals that are canonical with respect to  $N-1$  orbitals  $\Psi_j$  for  $j = 1 \dots N$  with  $j \neq i$ . These MO's have been called precanonical molecular orbitals (PCMO's). In our case, the key elements are the interaction parameters between the PCMO's of  $\pi$  type (see second column of Figure 4) and the PCMO's of  $\sigma$ -type mainly localized in the four-membered ring moiety of 4 (fourth column of Figure 4). It was, in fact, found that the PCMO's that transform according to  $b_1$  interact quite strongly ( $\langle b_1(\pi) | F | b_1(\sigma) \rangle = -2.34 \text{ eV}$ ), while interaction between the PCMO's of  $E$  symmetry is moderate. The calculated matrix elements, listed in the last column of Figure 4, were derived by using an INDO type<sup>25</sup> calculation.

**Electronic Absorption Spectra of 4 and 5.** The electronic absorption spectrum of 4 shows two bands at 315 and 224 nm (Figure 5), while that of 5 shows only one band above 200 nm, viz. at 284 nm, with vibrational spacings. The band in the electronic spectrum of 5 shows close similarities with respect to energy, intensity, and fine structure relative to that seen in the spectra of 10 and 11.<sup>21,22</sup> Since polarization measurements and MO calculations on 10 yield a  $\pi^* \leftarrow \pi$  transition for the first absorption band,<sup>21</sup> the same assignment for the first band of 5 seems reasonable. To assign the two bands in the electronic absorption spectrum of 4, CNDO/s-CI calculations<sup>26</sup> have been performed with adoption

(23) Heilbronner, E.; Schmelzer, A. *Helv. Chim. Acta* **1975**, *58*, 936.

(24) Edmiston, C.; Ruedenberg, K. *Rev. Mod. Phys.* **1963**, *35*, 457; *J. Chem. Phys.* **1965**, *43*, 597.

(25) Böhme, M. C.; Gleiter, R. *Theor. Chim. Acta* **1981**, *59*, 127.

Table III. Observed and Calculated Absorption Spectral Data of 4, 5, and 17

compd	band	observed		calculated (CNDO/s-CI)		
		$\lambda_{\max}$ , nm	$\nu/10^3$ , $\text{cm}^{-1}$	$\epsilon$	$\nu/10^3$ , $\text{cm}^{-1}$	predominant configuration
4	A	315	31.7	3120	34.57	$8e \leftarrow 2b_1$ (98%)
		230 (sh)	43.5	6700	46.30	$8e \leftarrow 7e$ (40%), $2a_2 \leftarrow 2b_1$ (54%)
5	B	224	44.6	9050	46.71	$8e \leftarrow 1a_2$ (90%)
		310	32.3	1920		
		296	33.8	3840		
		284	35.2	4140	36.87	$8b_1 \leftarrow 4a_2$ (98%)
		273	36.6	3180		
		265	37.7	2100		
17	A	255	39.2	1320		
		319	31.4	1090	40.08	$8b_2(\pi^*) \leftarrow 3a_2(\pi)$ (97%)
		305	32.8	2210		
		292	34.3	2350		
		280	35.7	1880		
	B	267	37.5	5330		
		256	39.1	6910	44.20	$8b_1(\pi^*) \leftarrow 3a_2(\pi)$ (95%)
		246	40.6	5630		
		237	42.2	4530		
		C (sh)	220	45.5	5880	49.52
214	46.7		6740			
207	48.3		7130			

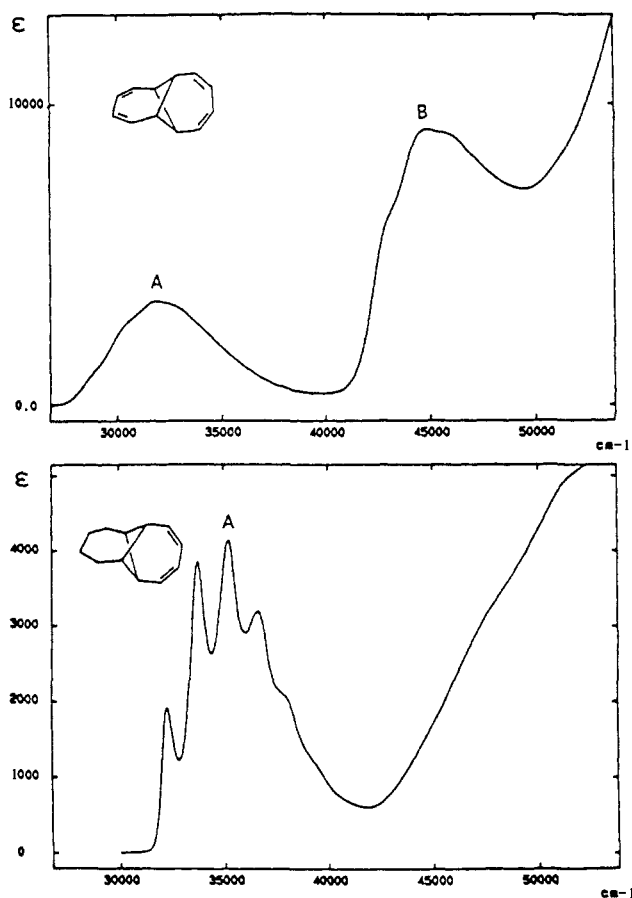
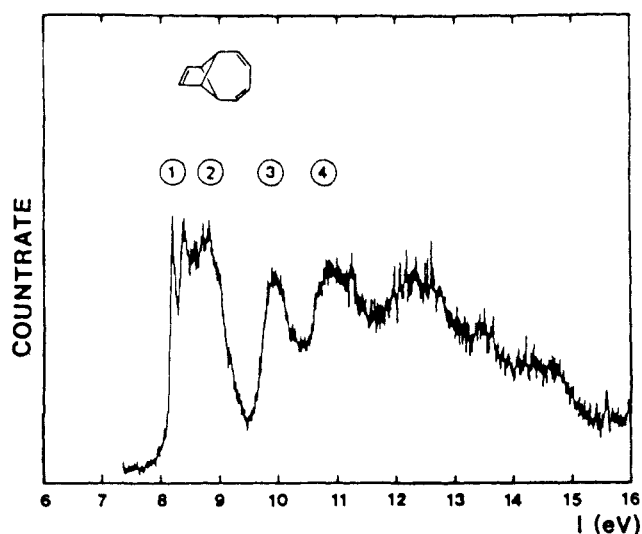


Figure 5. Electronic absorption spectra of 4 and 5 in cyclohexane.

of the prescribed MINDO/3-derived geometrical parameters. Only singly excited configurations involving the highest eight occupied and lowest eight unoccupied MO's have been considered. The results of these calculations are compiled in Table III. For 4, a first band is predicted at 289 nm arising from an  $8e(\pi^*) \leftarrow 2b_1(\pi)$  transition. Two close-lying transitions at 216 and 214 nm are predicted for the second band. The latter one is best described as the  $8e(\pi^*) \leftarrow 1a_2(\pi)$  transition, while in the other one, two configurations ( $8e(\pi^*) \leftarrow 7e(\pi)$  and  $2a_2(\pi^*) \leftarrow 2b_1(\pi)$ ) are the

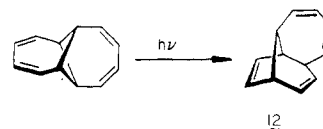
(26) Jaffe, H. H. *Acc. Chem. Res.* **1969**, *2*, 136. A modified version of the computer program written by Baumann, H. (*QCPE* **1977**, *10*, 333) was used.

(27) Mataga, N.; Nishimoto, K. *Z. Phys. Chem.* **1957**, *13*, 140.

Figure 6. He ( $I_{\alpha}$ ) PE spectrum of 13.

major contributors. If the interpretation suggested by the calculations is adopted, some uncertainty remains with regard to assigning the  $8e(\pi) \leftarrow 1a_2(\pi)$  transition. Thus, the measured split  $\Delta E$  between the  $8e(\pi^*) \leftarrow 2b_1(\pi)$  and  $8e(\pi^*) \leftarrow 1a_2(\pi)$  is uncertain by about  $1000 \text{ cm}^{-1}$  (0.13 eV).

Assignment of the first band in the electronic absorption spectrum of 4 to  $8e(\pi) \leftarrow 2b_1(\pi)$  is helpful in understanding the observed light-induced rearrangement of 4 to tricyclo[5.5.0.0<sup>4,8</sup>]dodeca-2,5,9,11-tetraene (12).<sup>18</sup> The excitation of an electron from  $2b_1$  will reduce the C-C bond strength in the four-membered ring, and these C-C bonds are therefore weakened in the first excited state.

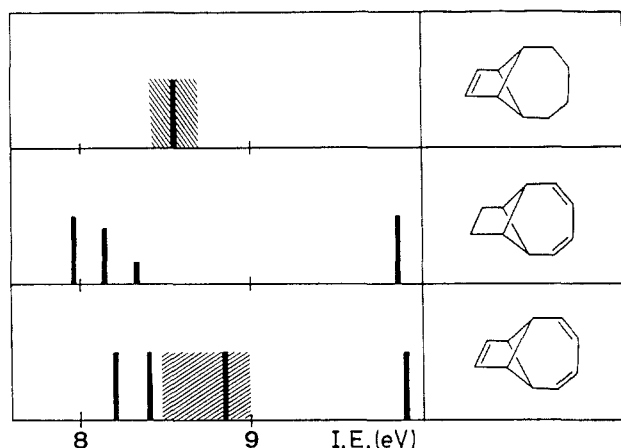


**PE Spectroscopic Analysis of 13.** The recent synthesis of tricyclo[5.3.0.0<sup>2,8</sup>]decatriene (13)<sup>28</sup> has also allowed study of the PE spectrum of a system with two mutually perpendicular  $\pi$  systems of different size. For reasons of symmetry, interactions only between the  $\pi^*$  orbitals of one  $\pi$  unit and the  $\pi$  orbitals of the other are expected. Although the cyclobutane unit is a powerful relay, the large energy difference between such bonding

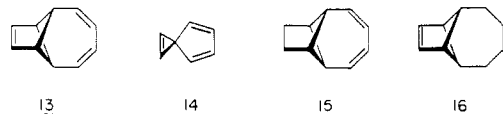
(28) Dressel, J.; Paquette, L. A. *J. Am. Chem. Soc.* **1987**, *109*, 2857.

**Table IV.** Comparison between the First Vertical Ionization Energies ( $I_{v,j}$ ) of **13** and **17** with Calculated Orbital Energies ( $\epsilon_j$ ) Based on FMO, MINDO/3, and ab Initio (STO-3G) Procedures<sup>a</sup>

compd	band	$I_{v,j}$	assignment	$-\epsilon_j$ (FMO)	$-\epsilon_j$ (MINDO/3)	$-\epsilon_j$ (STO-3G)
		8.21				
<b>13</b>	1	8.4	2a <sub>2</sub>	8.08	8.50	6.56
	2	8.8	7b <sub>2</sub>	8.67	8.80	7.44
	3	9.7	5b <sub>1</sub>	10.03	9.67	9.21
	4	10.6	6b <sub>2</sub>		10.36	10.57
<b>17</b>	1	8.17	3a <sub>2</sub>	8.06	8.28	6.29
	2	9.28	2a <sub>2</sub>	8.50	9.36	7.62
	3	10.1	7b <sub>2</sub>	10.60	9.64	9.40
	4	10.5	7b <sub>1</sub>	10.60	9.74	9.32
	5	11.0	13a <sub>1</sub>		9.84	10.24

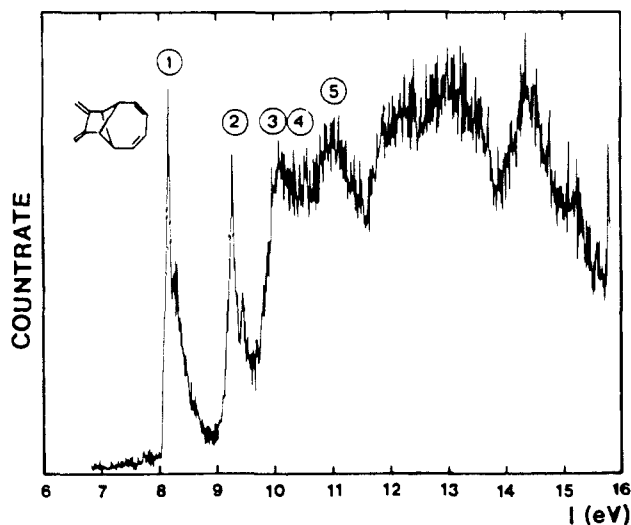
<sup>a</sup> All values are in electronvolts.**Figure 7.** Comparison between the first bands in the PE spectra of **13**, **15**, and **16**.

and antibonding niveaus were expected to give rise only to small, if not negligible, effects. A similar case has been encountered during study of the interactions in a derivative of spiro[4.2]heptatriene (**14**).<sup>29</sup> In **14**, the expected through-space interaction



between  $\pi^*$  of the ethylene unit and  $\pi(a_2)$  of the butadiene component could not be detected. Instead,  $\pi-\sigma^*$  interaction led to destabilization of  $a_2(\pi)^2$ . In the PE spectrum of **13** (Figure 6, Table IV), one broad peak is seen around 8.5 eV (bands 1 and 2) well separated from a second band at 9.9 eV. The first peak, assigned to two close-lying bands, shows a steep onset with fine structure (8.2, 8.4 eV), while the second has a Gaussian shape (8.8 eV).

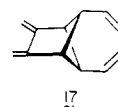
For suitable analysis of the first three bands, the PE spectrum of **13** is compared with that of tricyclo[5.3.0.0<sup>2,8</sup>]dec-9-ene (**16**)<sup>30</sup> in tandem with the results of MO calculations. For the latter, we again applied a semiempirical procedure (MINDO/3),<sup>19</sup> an SCF method on the Hartree-Fock level with a minimum basis (STO-3G),<sup>20</sup> and an empirical procedure using a fragment molecular orbital (FMO) approach. Figure 7 represents in bar-graph fashion the first bands of the PE spectra of **13**, **15**, and **16**. This comparison shows that the PE spectrum of **13** can be derived from those of **15** and **16** by superposition. The close similarity shows up as well in the shape of the first two bands. The first band in the PE spectrum of **13** ( $2a_2, \pi$ ) shows a fine structure similar to

**Figure 8.** He ( $I_a$ ) PE spectrum of **17**.

that in the PE spectrum of **15**. The second band in the PE spectrum of **13** ( $7b_2, \pi$ ) resembles a great deal the  $\pi$  band in the spectrum of **16**. The difference in the ionization energies between the three PE spectra can be ascribed to the inductive contributions of the additional  $sp^2$  centers in **13** relative to **15** and **16**.

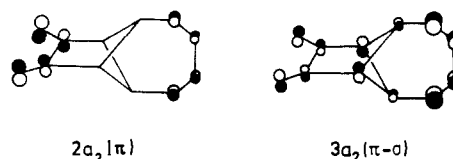
The qualitative picture recorded in Figure 7 is fully confirmed by the results of the calculations listed in Table IV. The calculations for **13** are based on the geometrical parameters derived by the MINDO/3 method wherein the degrees of freedom of **13** were minimized by assuming  $C_{2v}$  symmetry. Only a minute  $2a_2(\pi)-3a_2(\pi^*)$  interaction (<0.1%) was encountered as anticipated. However, a large interaction exists between the four-membered ring and  $\pi$  units. In the FMO model, this interaction is nicely accommodated by a resonance integral of -1.9 eV. The adopted basis energies are (ethylene) = -9.6 eV, (*cis*-butadiene) = -8.4, -10.9 eV, (cyclobutane) = -11.1 and -12.5 eV.

**Comparative Photoelectron Spectroscopic Response of 17.** The general approach for the synthesis of **4** and **13** also permitted the synthesis of **17**.<sup>28</sup> In this isomer of **4**, the 1,4-positions of one butadiene moiety are relay-connected with the 2,3-position of the other perpendicularly oriented fragment. This difference in connectivity lowers the symmetry from  $D_{2d}$  (**4**) to  $C_{2v}$  (**17**).



The PE spectrum of **17** (see Figure 8) has an appearance similar to that of **4**. Also revealed are two sharp bands below 10 eV followed by a first series of strongly overlapping bands between 10 and 11.5 eV. The recorded vertical ionization energies of **17** are listed in Table IV.

The interaction scheme discussed for **4** holds in principle for **17**. Thus, the first band corresponds to ionization from the antibonding linear combination between the Walsh-type orbital of  $A_2$  symmetry of the central ring with the HOMO's of the two butadiene fragments. For the second band, essentially no  $\sigma$  participation is expected. The corresponding wave functions are shown schematically below.



The assignment given in Table IV is substantiated by MO calculations using the FMO approach as outlined for **4**, the MINDO/3 method,<sup>19</sup> and a minimum basis (STO-3G) ab initio procedure.<sup>20</sup> All three calculations predict  $3a_2(\pi-\sigma)$  and  $2a_2(\pi)$

(29) Bischof, P.; Gleiter, R.; Dürr, H.; Ruge, B.; Herbst, P. *Chem. Ber.* **1976**, *109*, 1412.

(30) Gleiter, R.; Zimmerman, H., unpublished results.

(31) Paquette, L. A.; Dressel, J.; Pansegrau, P. D. *Tetrahedron Lett.* **1987**, *28*, 4965.

to lie above close-lying Walsh-type orbitals.

Proper comparison between the first bands of the PE spectra of isomers **4** and **17** shows a considerably higher energy for the first band of **17** in relation to that of **4** ( $I_1(\mathbf{17}) - I_1(\mathbf{4}) = 0.6$  eV) and a smaller split between  $I_1$  and  $I_2$  for **17** (1.1 eV) as compared to **4** (1.4 eV). This latter observation can be traced back to the size of the AO coefficients of the  $\pi$  wave functions of the butadiene moiety. In the HMO model, the coefficients at the 1- and 4-positions are predicted to be 0.602, while the AO coefficients at the 2- and 3-positions amount to 0.372.

In the FMO approach, this yields two different values for the interaction parameter:

$$\begin{aligned} \text{1,4 connection: } H_{\pi,w} &= \langle \psi_2 | H | \Phi_w \rangle = \\ & 2 \times 0.5 \times 0.602 \langle p_\pi | H | p_w \rangle = -1.144 \text{ eV} \end{aligned}$$

$$\begin{aligned} \text{2,3 connection: } H_{\pi,w} &= \langle \psi_2 | H | \Phi_w \rangle = \\ & 2 \times 0.5 \times 0.372 \langle p_\pi | H | p_w \rangle = -0.707 \text{ eV} \end{aligned}$$

**Electronic Absorption Spectrum of 17.** The electronic absorption spectrum of **17** shows two bands at 292 and 256 nm and a shoulder at 210 nm. The two bands show considerable fine structure (see Table III). To assign the bands in the spectrum, we have performed CNDO/s-CI calculations<sup>26</sup> on **17** while adopting those structural parameters obtained by MINDO/3 calculations. Only singly excited configurations involving the eight highest occupied and eight lowest unoccupied MO's have been considered. The results of these calculations are listed in Table III. The first band is predicted to appear at 249.5 nm and the second one at 226.2 nm. In a fairly good approximation, the first two excited states can each be described by a single electronic transition,  $8b_2(\pi^*) \leftarrow 3a_2(\pi)$  and  $8b_1(\pi^*) \leftarrow 3a_2(\pi)$ , respectively. Consequently, the two transitions originate from the HOMO and terminate in the two lowest unoccupied MO's. The LUMO,  $8b_2(\pi^*)$ , is mainly centered at positions 3-6, i.e., at the *endo*-butadiene moiety while  $8b_1(\pi^*)$  is localized at the *exo*-butadiene fragment.

As discussed for **4**, the promotion of an electron from  $3a_2(\pi - \sigma)$  to  $8b_2(\pi^* + \sigma^*)$  will reduce the C-C bond strength of the four-membered ring in **17** and thus a light-induced rearrangement in the first excited state of this compound may occur.

## Discussion

The most interesting observation in our examination of **4** is the close similarity of the energy gaps [ $\Delta I(1,2) = 1.44$  eV and  $\Delta E(1,2) = 1.60$  eV] between the corresponding bands in its PE ( $I$ ) and electron absorption ( $E$ ) spectra. A similar equivalence has been observed for **3**.<sup>7</sup> To understand this equivalence, the valence orbitals of the two perpendicular  $\pi$  systems and the cyclobutane ring need to be defined (see Figure 9). The coefficients of the AO's of the butadiene moieties are those derived from an HMO calculation. The resulting linear combinations are

$$\psi_1(a_2) = 1/\sqrt{2} (\phi_{cb} + \phi_{cb'}) \quad (1)$$

$$\psi_2(b_1) = 1/\sqrt{2} (\phi_{cb} - \phi_{cb'}) \quad (2)$$

The corresponding energy levels are nearly degenerate due to their large separation in space. For the doubly degenerate wave functions  $\phi_k$  and  $\phi_{k'}$  (corresponding to  $\epsilon_k$  and  $\epsilon_{k'}$ , Figure 9), which transform according to  $E$  in  $D_{2d}$ , we have used the localized representation as given in Figure 9. The two  $\sigma$  orbitals of the cyclobutane ring are denoted as  $\phi_\sigma$  and  $\phi_{\sigma^*}$ . The former transforms according to  $b_1$  and the latter according to  $a_2$  (see Figure 9). Both are ideally suited to interact with the corresponding linear combinations of the two highest occupied  $\pi$  MO's, giving rise to the following linear combinations:

$$\phi_i(a_2) = C_1\psi_1 + C_2\phi_{\sigma^*} \quad (3)$$

$$\phi_j(b_1) = C'_1\psi_2 - C'_2\phi_\sigma \quad (4)$$

As concerns the energy difference between the first two ionization energies  $I_{v,1}$  and  $I_{v,2}$ , Koopmans' approximation<sup>4</sup> has been adopted.

$$\Delta I(1,2) = -\epsilon_i + \epsilon_j \quad (5)$$

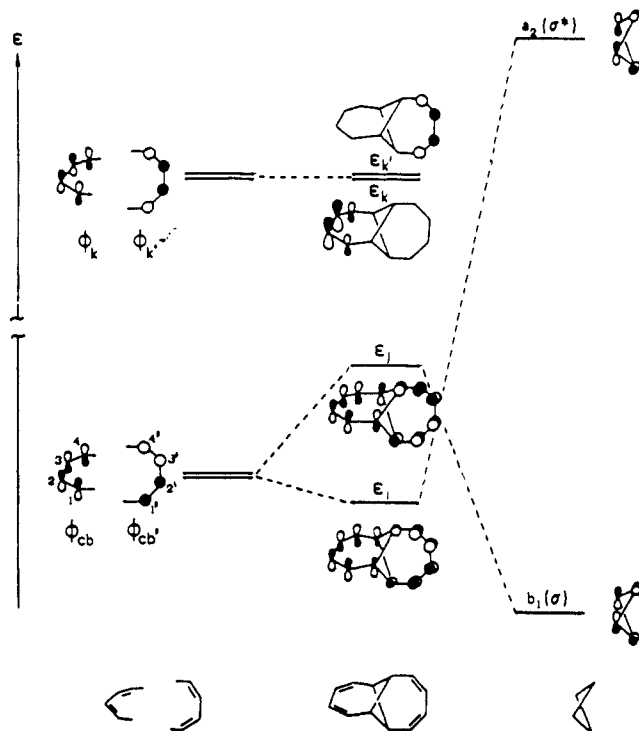


**Figure 9.** Definition of valence orbitals of the two perpendicular  $\pi$  MO's and the  $\sigma$  MO's of the four-membered ring in **4** ( $D_{2d}$ ).

In order to deal with the energy difference between the first two singlet excited states, the following equations can be written if one assumes that the electron is promoted from  $\epsilon_j$  to  $\epsilon_k$  and from  $\epsilon_i$  to  $\epsilon_{k'}$ :

$$E_{j \rightarrow k} = \epsilon_k - \epsilon_j - J_{jk} + 2K_{jk} \quad (6)$$

$$E_{i \rightarrow k} = \epsilon_k - \epsilon_i - J_{ik} + 2K_{ik} \quad (7)$$

where  $J_{rk}$  (Coulomb integral) and  $K_{rk}$  (exchange integral) have their usual meaning. From (6) and (7), the energy difference,  $\Delta E(1,2)$ , between the first two excited singlet states can be derived:

$$\Delta E(1,2) = -\epsilon_i + \epsilon_j - (J_{ik} - J_{jk}) + 2(K_{ik} - K_{jk}) \quad (8)$$

$$\Delta E(1,2) = -\epsilon_i + \epsilon_j - \Delta J + \Delta K \quad (9)$$

After substitution of the expressions for  $J$  and  $K$  in (8) and adopting the ZDO approach,  $\Delta J$  and  $\Delta K$  are expressed as

$$\Delta J = 1/2 (C_1^2 - C_1'^2)(J_{cb,k} + J_{cb',k} - 2J_{\sigma,k}) \quad (10a)$$

$$\Delta K = (C_1^2 - C_1'^2)K_{cb,k} \quad (10b)$$

The difference  $\Delta$  between the energies  $\Delta I(1,2)$  and  $\Delta E(1,2)$  results:

$$\Delta = \Delta J - \Delta K \quad (11)$$

$$\Delta = 1/2 (C_1^2 - C_1'^2)(J_{cb,k} + J_{cb',k} - 2J_{\sigma,k} - 2K_{cb,k}) \quad (12)$$

Three cases for which the difference ( $\Delta$ ) is equal or nearly equal to zero can be visualized:

(i) The first factor of (12) is equal to zero

$$C_1^2 - C_1'^2 = 0 \quad (13)$$

This means that the energy separation between  $\epsilon_{cb}(\epsilon_{cb'})$  and  $\epsilon_\sigma$  is equal to that between  $\epsilon_{cb}(\epsilon_{cb'})$  and  $\epsilon_{\sigma^*}$ . As a result, one obtains

$$\Delta J = 0 \text{ and } \Delta K = 0 \quad (14)$$

as in the case of **3**.<sup>7</sup> Semiempirical calculations of the MNDO, MINDO/3, and EH type do not agree with this condition.

(ii) The second factor of (12) is equal to zero. To estimate this, the sum of the Coulomb integrals needs to be considered. The values of  $J_{cb',k}$  and  $J_{\sigma,k}$  are smaller than those of  $J_{cb,k}$  because the

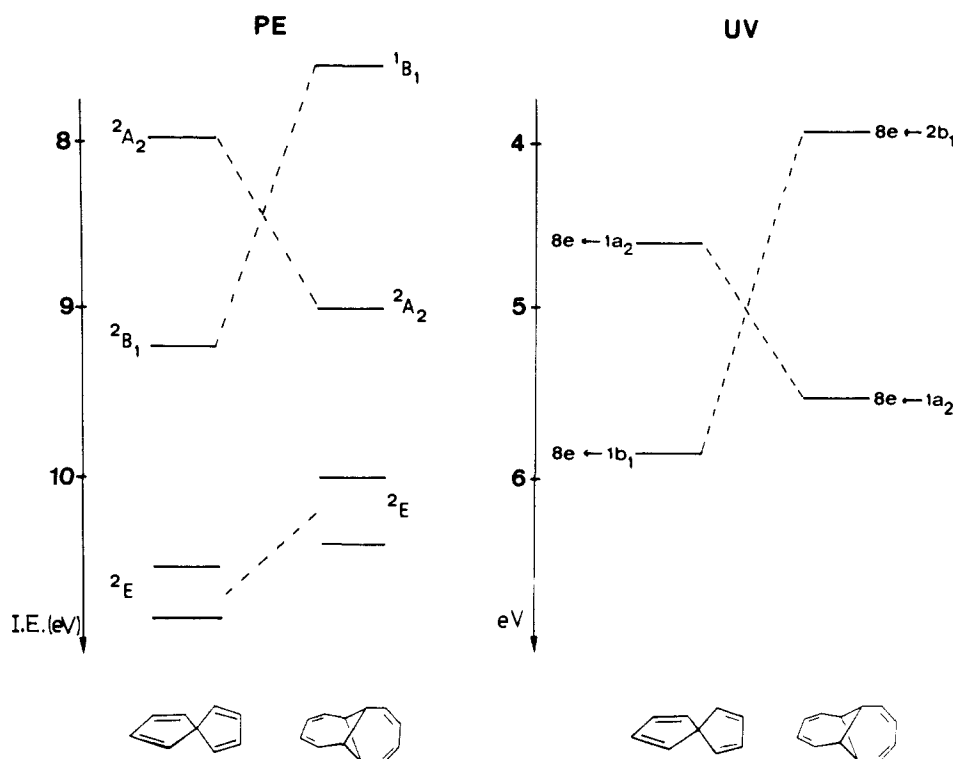


Figure 10. Comparison between the first PE and UV bands of 3 and 4.

former ones do not contain the one-center repulsion integrals and the electrons in orbitals  $\phi_{cb}$  and  $\phi_{\sigma}$  are far away from that in  $\phi_k$  (see Figure 9). Thus, one can expect:

$$J_{cb,k} + J_{cb',k} - 2J_{\sigma,k} < 0 \quad (15)$$

From the fact that  $K_{cb,k} > 0$ , it follows that

$$\Delta J > 0 \text{ and } \Delta K > 0 \quad (16)$$

In order to have  $\Delta \approx 0$ , the following condition must hold

$$\Delta J \approx \Delta K \quad (17)$$

The MINDO/3 results summarized below show that this equation does not hold.

(iii) The third condition is that both factors of (12) are small. It will be shown below that this possibility is the most likely one. Using MINDO/3 results as a guide, we find  $J_{ik} - J_{jk} = 0.006$  eV and  $K_{ik} - K_{jk} = 0.16$  eV. From these values, it follows that  $\Delta = 2(K_{jk} - K_{ik}) = -0.32$  eV [see (8), (9), and (11)].

By making recourse to the wave functions of the MINDO/3 calculations, the first factor of (12) can be calculated. The MINDO/3 method predicts that the 2p AO coefficients of the cyclobutane moiety in the two highest occupied MO's  $\phi_i(a_2)$  and  $\phi_j(b_1)$  are 0.072 and 0.227, respectively. From (3) and (4), it can be determined that  $C'_2 = 0.454$  and  $C_2 = 0.141$ , respectively. Thus, the extent to which orbitals  $\phi_{\sigma}$  and  $\phi_{\sigma^*}$  blend into orbitals  $\phi_j$  and  $\phi_i$  turns out to be 20.6% and 2.1%, respectively. The difference between the two contributions is therefore

$$C_2'^2 - C_2^2 = C_1'^2 - C_1^2 = 0.185 \quad (18)$$

The second factor in (12), the sum of the  $J$  and  $K$  values, can be calculated by using the Nishimoto–Mataga approximation.<sup>27</sup> In combination with the wave functions for  $\pi$  and  $\sigma$  as defined above, it is found that

$$1/2 (J_{cb,k} + J_{cb',k} - 2J_{\sigma,k} - 2K_{cb,k}) = -1.332 \text{ eV} \quad (19)$$

$$\Delta = 0.185(-1.332) \text{ eV} = -0.25 \text{ eV} \quad (20)$$

a value that is close to that derived by the MINDO/3 method.

The calculations carried out to assign the first bands in the electronic absorption spectrum of 17 (see Table III) clearly indicate

that the energy difference between the first two bands,  $\Delta E(1,2)$ , corresponds approximately to the energy difference of the LUMO's,  $8b_2(\pi^*)$  and  $8b_1(\pi^*)$ , because both excited states originate from the HOMO ( $3a_2(\pi)$ ). The excited state corresponding approximately to the transition  $8b_2(\pi^*) \leftarrow 2a_2(\pi)$  is predicted at  $51\,800 \text{ cm}^{-1}$  and thus is beyond our experimental reach.

### Conclusion

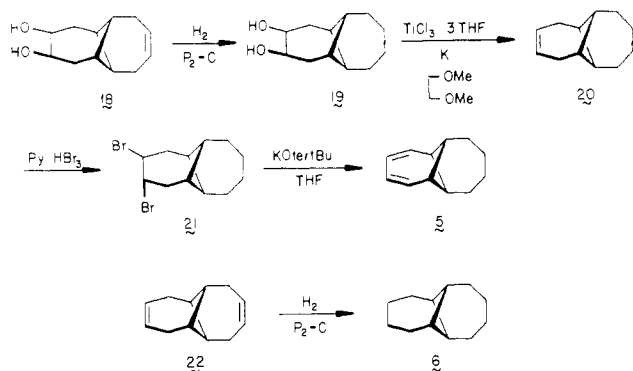
Our investigations show a very large interaction between the two perpendicular  $\pi$  systems in 4 via its central four-membered ring system. The calculated orbital sequence and the PE bands suggest the sequence  $2b_1$  above  $1a_2$ . A direct comparison between the first bands in the PE and electronic absorption spectra of 3 and 4, shown in Figure 10, demonstrates the larger interaction in 4. This indicates that the "relay conjugation" in 4 is more efficient than the spiroconjugation<sup>9</sup> in 3.

Although a correspondence between  $\Delta E(1,2)$  and  $\Delta I(1,2)$  has been found in 3 and 4, the explanation for both cases differs. In 3, the equality of  $\Delta I(1,2)$  with  $\Delta E(1,2)$  is the consequence of spiroconjugation<sup>9</sup> between two identical  $\pi$  systems perpendicularly arranged to each other. Due to the high symmetry of the system, the Coulomb repulsions and the exchange contributions to  $\Delta$  are zero within a first-order approximation. In 4, however, the interaction between  $b_1(\pi)$  and  $b_1(\sigma)$  is not identical with  $a_2(\pi)$  and  $a_2(\sigma^*)$ .<sup>8,10</sup> The contribution of this difference to the Coulomb repulsion and exchange integrals in  $\Delta$  is, however, small, and thus the difference between  $\Delta I(1,2)$  and  $\Delta E(1,2)$  also resides within experimental error in this instance.

A strong interaction between the two perpendicular  $\pi$  systems and the central four-membered ring similar to that in 4 is found for 17. The difference between both PE spectra can be traced back to the different connectivity of the butadiene units to the four-membered ring. Due to the similar (0.372) AO coefficients at positions 2 and 3 of the HOMO of butadiene compared to positions 1 and 4 (0.602), a smaller energy gap between the first two PE bands results in 17.

The origin of the energy difference of the first two bands in the electronic absorption spectrum of 17 is totally different from that of 4. In 17, the energy difference is mainly due to the splitting of the lowest unoccupied MO's. This can be traced back to the lower symmetry of 17 as compared to 4.

Scheme I



### Experimental Section

Hydrocarbons **5** and **6** were prepared by the series of reactions summarized in Scheme I.

**cis-Tricyclo[5.5.0.0<sup>2,8</sup>]dodecane-4,5-diol (19).** Diol **18** (0.58 g, 3.0 mmol) was dissolved in hot methanol (10 mL) in a 50-mL Schlenk flask. Under argon, 116 mg of 5% palladium on carbon was added, and the black suspension was stirred vigorously under hydrogen in an atmospheric hydrogenator for 1.3 h until no starting material was left according to TLC. The mixture was filtered through Celite, and the filter residue was washed with tetrahydrofuran to afford 0.58 g (99%) of **19** as a white solid, mp 167–170 °C, after rotary evaporation: <sup>1</sup>H NMR (300 MHz, CDCl<sub>3</sub>) δ 4.23 (t, *J* = 5.4 Hz, 2 H), 2.63–2.57 (m, 1 H), 2.05–1.89 (series of m, 9 H), 1.73–1.50 (series of m, 8 H); <sup>13</sup>C NMR (75 MHz, CDCl<sub>3</sub>, ppm) 73.94, 40.82, 40.10, 38.32, 35.16, 30.50, 25.22, 25.12; MS, *m/z* (M<sup>+</sup>) calcd 196.1464, obsd 196.1471.

**Tricyclo[5.5.0.0<sup>2,8</sup>]dodecane-4-ene (20).** Titanium trichloride tris(tetrahydrofuran) complex (13 g, 35 mmol), potassium (5.4 g, 0.14 mol), and anhydrous dimethoxyethane (100 mL) contained in a 250-mL Schlenk flask fitted with a reflux condenser was heated at the reflux temperature for 1.25 h. Diol **19** (0.56 g, 2.9 mmol) was added in 20 mL of anhydrous dimethoxyethane, and reflux was resumed for 25.5 h. The cooled reaction mixture was diluted with petroleum ether (100 mL) and filtered through Celite. The black pyrophoric residue was rinsed with pentane (100 mL), the combined organic phases were washed with water (200 mL), and the aqueous layer was extracted with petroleum ether (50 mL). The combined organic phases were washed with water (2 × 100 mL) and brine (50 mL), dried, evaporated (150–160 mmHg, room temperature), evacuated (20 mmHg, room temperature, 10 min), and distilled bulb-to-bulb (0.03 mmHg, 30–40 °C, receiver cooled to –78 °C) to give 0.36 g (78%) of **20** as a clear, colorless oil with a faint olefinic odor: IR (neat, cm<sup>-1</sup>) 3000, 2910, 2840, 2810; <sup>1</sup>H NMR (300 MHz, CDCl<sub>3</sub>) δ 5.56 (br s, 2 H), 2.30–2.23 (m, 4 H), 2.10 (br s, 2 H), 1.99 (br s, 2 H), 1.76–1.70 (m, 4 H), 1.62–1.56 (m, 4 H); <sup>13</sup>C NMR (75 MHz, CDCl<sub>3</sub>, ppm) 125.86, 40.71, 38.46, 33.92, 30.25, 25.46; MS, *m/z* (M<sup>+</sup>) calcd 162.1417, obsd 162.1413.

**trans-4,5-Dibromotricyclo[5.5.0.0<sup>2,8</sup>]dodecane (21).** A mixture of **20** (0.35 g, 2.2 mol), pyridinium bromide perbromide (0.74 g, 2.4 mmol), glacial acetic acid (10 mL), and carbon tetrachloride (10 mL) was stirred at room temperature for 2.3 h and then diluted with more carbon tetrachloride (10 mL). The suspension was sequentially washed with water (20 mL), aqueous sodium sulfite solution (10 mL), and saturated aqueous

sodium bicarbonate solution (10 mL). The colorless, clear organic phase was dried, filtered, and evaporated. A volatile nonpolar impurity was removed by MPLC (silica gel, petroleum ether) to give 0.57 g (80%) of **21** as a pale yellow solid: mp 64.0–65.0 °C; IR (CDCl<sub>3</sub>, cm<sup>-1</sup>) 2910, 2850, 2840, 1435; <sup>13</sup>C NMR (300 MHz, CDCl<sub>3</sub>) δ 4.64–4.50 (m, 2 H), 2.80–2.68 (m, 2 H), 2.30–2.15 (m, 2 H), 2.06–1.95 (m, 5 H), 1.73–1.46 (2 br s, 8 H); <sup>13</sup>C NMR (75 MHz, CDCl<sub>3</sub>, ppm) 57.49, 42.98, 40.07, 39.98, 29.77, 24.89; MS, *m/z* (M<sup>+</sup>) calcd 321.9754, obsd 321.9728.

**Tricyclo[5.5.0.0<sup>2,8</sup>]dodecane-3,5-diene (5).** Under argon, a solution of dibromide **21** (0.48 g, 1.5 mmol) in anhydrous tetrahydrofuran (2 mL) was treated with 1.6 M potassium *tert*-butoxide in tetrahydrofuran (3.8 mL, 6 mmol) at room temperature. After 3 h of stirring, the brown-orange reaction mixture was partitioned between pentane (20 mL) and water (20 mL). The aqueous phase was extracted with pentane (10 mL), and the combined organic phases were washed with water (2 × 10 mL) and brine (10 mL) and evaporated (60 mmHg, room temperature). The residue was evacuated (20 mmHg, room temperature, 10 min) and then distilled twice in a Kugelrohr apparatus (0.05 mmHg, 50 °C, receiver cooled with dry ice–2-propanol) to give 200 mg (83%) of **5** as a colorless oil, homogeneous by GC: IR (neat, cm<sup>-1</sup>) 3015, 2980, 2850, 2830; <sup>1</sup>H NMR (300 MHz, CDCl<sub>3</sub>) δ 6.26–6.14 (m, 2 H), 5.83–5.75 (m, 2 H), 2.48 (br d, *J* = 6.9 Hz, 2 H), 2.15–2.07 (m, 2 H), 1.79–1.63 (2 m, 8 H); <sup>13</sup>C NMR (75 MHz, CDCl<sub>3</sub>, ppm) 137.77, 123.23, 40.91, 33.24, 30.33, 24.97; MS, *m/z* calcd 160.1260, obsd 160.1256. Anal. Calcd for C<sub>12</sub>H<sub>16</sub>: C, 89.94; H, 10.06. Found: C, 89.69; H, 10.12.

**Tricyclo[5.5.0.0<sup>2,8</sup>]dodecane (6).** A 50-mL Schlenk flask containing diene **22** (224 mg, 1.40 mmol) and 5% palladium on carbon (118 mg) was evacuated, flushed with argon, and charged with methanol. After 1 h of vigorous stirring in an atmospheric hydrogenator, capillary GC showed that no starting diene remained. After the mixture had settled for 24 h, the supernatant solution was decanted and filtered through a cotton plug. The granular black residue was washed with distilled pentane (30 mL), and the combined filtrates were washed with water (20 mL). The aqueous phase was extracted with pentane (2 × 10 mL), and the combined pentane phases were washed with water (2 × 10 mL) and brine (10 mL) and rotary evaporated (60 mmHg, room temperature). The remaining colorless oil was taken up in pentane (2 mL), dried, filtered, rotary evaporated, and distilled in a Kugelrohr apparatus after evacuation (10 min, 20 mmHg, room temperature; and then 0.05 mmHg, 50 °C, receiver bulb cooled to –78 °C) to yield 214 mg (93%) of **6**, a white solid that melted below room temperature: IR (CDCl<sub>3</sub>, cm<sup>-1</sup>) 2915, 2865, 2845, 1465, 1455, 1440; <sup>1</sup>H NMR (300 MHz, CDCl<sub>3</sub>) δ 2.05–1.98 (m, 4 H), 1.73–1.63 (m, 8 H), 1.63–1.50 (m, 8 H); <sup>13</sup>C NMR (75 MHz, CDCl<sub>3</sub>, ppm) 40.08, 30.55, 25.46; MS, *m/z* (M<sup>+</sup>) calcd 164.1565, obsd 164.1599. Anal. Calcd for C<sub>12</sub>H<sub>20</sub>: C, 87.73; H, 12.27. Found: 87.54; H, 11.99.

**Photoelectron and Ultraviolet Spectroscopic Measurements.** The He (*I*) PE spectra were recorded on a Perkin-Elmer PS-18 instrument at room temperature by using multiscanning techniques and electronic data acquisition with a Hewlett Packard HP 1000 computer. The absorption spectra of **4** and **5** were recorded in cyclohexane with a Cary 17D spectrometer.

**Acknowledgment.** Financial support in Heidelberg was provided by the Fonds der Chemischen Industrie and BASF Aktiengesellschaft. The work at Ohio State was supported by the National Science Foundation. A.T. is grateful to the Alexander von Humboldt Foundation for a stipend.